

Short Communication

Sulfur/Sisal Fiber Carbons Composites as Anode Materials for Lithium-ion Batteries

Rui Du^{1,2}, Zhangfa Tong¹, Chun Wei^{1,2}, Aimiao Qin^{2*}, Gaige Zhang²

¹ School of Chemistry and Chemical Engineering, Guangxi University, Nanning 530001, PR China

² Guangxi Ministry-Province Jointly-Constructed Cultivation Base for State Key Laboratory of Processing for Non-ferrous Metal and Featured Materials, Guilin University of Technology, Guilin 541004, PR China.

*E-mail: 317881264@qq.com

Received: 7 March 2017 / Accepted: 18 April 2017 / Published: 12 May 2017

The sulfur/sisal fiber carbons composites were prepared by pyrolysis and hydrothermal method. The structure of the sulfur/SFCs composites were characterized by X-ray diffraction and scanning electron microscopy, and the electrochemical performance of the sulfur/SFCs composites was tested by constant current charge-discharge tests. The initial discharge specific capacity of the sulfur/SFCs composites is 1223 mAhg⁻¹ and the reversible capacity of the sulfur/SFCs composites is about 400mAhg⁻¹. The charge-discharge efficiency closed to 90% after the first cycle.

Keywords: Sulfur, sisal fiber carbons, hydrothermal, anode materials

1. INTRODUCTION

Sulfur has considerable theoretical capacities, high initial coulombic efficiency and good safety which has been proposed as promising materials for the next generation of high-performance rechargeable lithium batteries due to their high theoretical capacity [1]. However, it exhibits low utilization and fast fades in lithium batteries due to their electrically and ionically insulated nature as well as solvent-solubility. Therefore, the sulfur must be well combined with a conductive agent when prepared as an electrode [2, 3].

Sisal is planted widely in Guangxi China. Sisal fiber is a major by-product in sisal industry. Sisal fibers have excellent mechanical property which are mainly used as textiles, artware and reinforced material [4-7]. Sisal fiber contains a large of carbon which posses high specific capacity and perform good electrochemical stability as anode materials for LIBs [8-11].

By pyrolysis of sisal fibers, a new microporous sisal fiber carbons (SFCs) were obtained [12, 13], and then the composites of sulfur/SFCs were prepared by simple hydrothermal method. As anode materials for LIBs, the sulfur/SFCs composites exhibited high specific capacity and excellent cycle stability.

2. EXPERIMENTAL

Sisal fibers carbons were prepared as the previous method [12].

The sulfur/SFCs composites were synthesized by hydrothermal method, 0.75g grounded SFCs were dispersed in 70mL mixed solution which contains 35mL $\text{Na}_2\text{S}_2\text{O}_3$ with concentration of 0.5mol/L and 35mL H_2SO_4 with concentration of 0.5mol/L. The mixture was stirred in an autoclave lined with PTFE of 100mL. The autoclave was heated to the temperatures of 200°C and with remains for 14 h. After cooling, the product was filtered and washed repeatedly with deionized water until pH=7. The final composites were obtained by drying at 80°C for 12h in a vacuum oven.

XRD test was performed on a PANalytical X'Pert PRO diffractometer with nickel-filtered Cu K α radiation. The data were recorded by the scattering angles (2θ) between 10° and 70° in steps of 0.05°. The morphology of the samples was examined by an Oxford S-4800 scanning electron microscope.

Electrochemical tests were conducted with CR2025-type coin cells with Li foil as counter electrode. Carbon electrodes were prepared by blade-coating a slurry containing 80 wt% of the composites, 10 wt% of polyvinylidene fluoride and 10 wt% of acetylene black dispersed in N-methyl-2-pyrrolidinone solvent on a copper foil and dried in a vacuum oven at 110°C for 12 h. The cells were assembled in an argon-filled glove box (VACMO40-1). The electrolyte was 1M LiPF_6 which was prepared by dissolving LiPF_6 in a mixture of ethylene carbonate, dimethyl carbonate and diethyl carbonate with a volume ratio of 1:1:1. Separator was the Celgard 2400 microporous polypropylene film. Charge-discharge tests were performed between 0.01 and 3.00V at a constant current density of 0.1 C using a Neware BTS battery test system.

3. RESULTS AND DISCUSSION

The XRD patterns of sulfur, SFCs and sulfur/SFCs composites are shown in Fig. 1. It can be seen that the sulfur in the sulfur/SFCs composite is amorphous. At 29(2 θ), the diffraction peak of the sulfur/SFCs composites disappears, which suggest that there may be some interaction between sulfur and SFCs. Compared with the XRD pattern of sulfur, the XRD spectra of the sulfur/SFCs composites do not exhibit the peak of sulfur, which demonstrates that the sulfur is in a highly dispersed state in the sulfur/SFCs composites [14]. Meanwhile, the diffraction peaks of graphitized carbon can not be seen, which suggests that SFCs are amorphous structure in the composites.

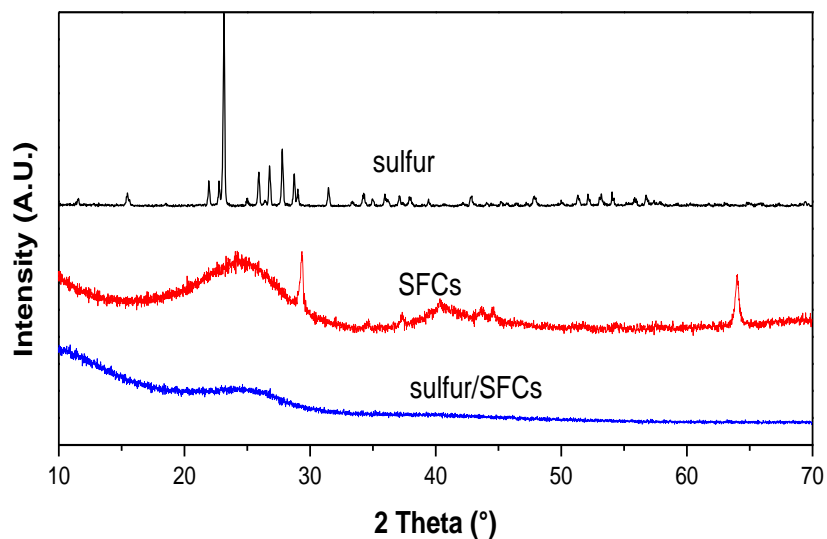


Figure 1. XRD patterns of sulfur, SFCs and sulfur/SFCs composites.

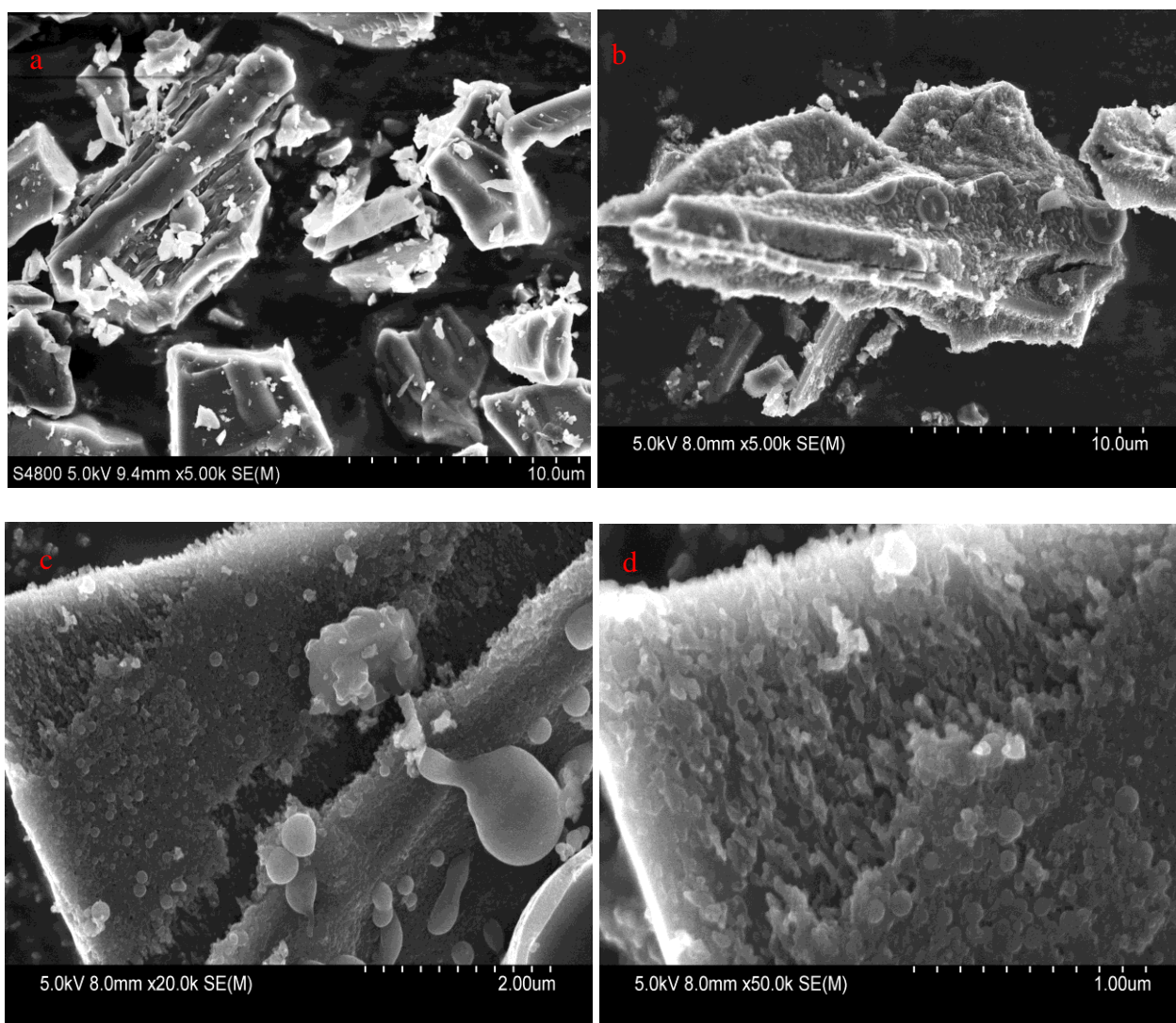


Figure 2. SEM images of SFCs (a), sulfur/SFCs (b, c, d)

The SEM images of the individual SFCs and the sulfur/SFCs composites are shown in Fig. 2. We can see that the SFCs (Fig. a) have no definite shape. For the sulfur/SFCs composites (Fig. a, b, c), thick coating of the sulfur is visible owing to the reaction between $\text{Na}_2\text{S}_2\text{O}_3$ and H_2SO_4 with hydrothermal process. It is obviously that the dimension of the sulfur/SFCs composites particles is larger than that of the SFCs particles. During the hydrothermal process, the synthesized sulfur nucleates into and onto the interior and surface of the SFCs. Most of the synthesized sulfur is exposed to the electrolyte during the electrochemical process [15].

Fig. 3(a) are the cycling performance of the sulfur/SFCs composites and the SFCs, which were tested in the voltage range of 0.01–3.00V at a constant current of 50 mA g^{-1} . It can be seen that the sulfur/SFCs composites possess the higher specific capacity of 1223 mAh g^{-1} for the first discharge, greatly exceeding that of the SFCs. The result was caused by the high theoretical specific capacity of the sulfur and the SFCs provide the conductive network for the sulfur in the process of charge-discharge. However, there is a serious capacity fade after the first discharge, which may be caused by the decomposition of electrolyte on the surface of the electrode and the solid electrolyte interphase (SEI) layer is formed [16].

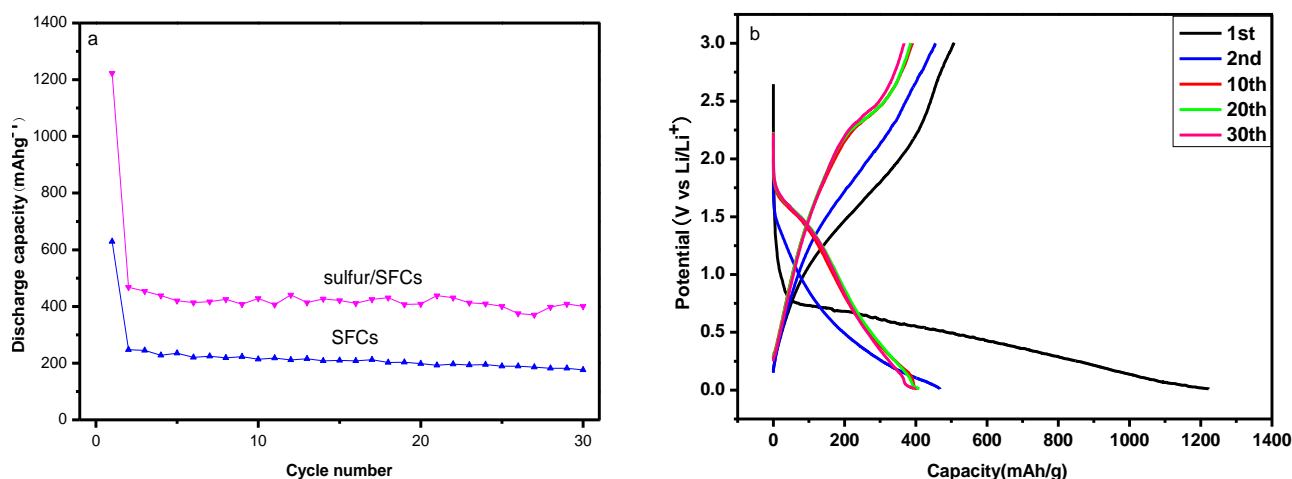
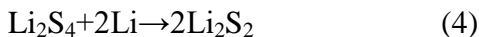


Figure 3. Cycling performance curves of the electrodes based on the sulfur/SFCs composites and the SFCs (a), the charge-discharge curves of the electrodes based on the sulfur/SFCs composites (b)

Charge-discharge curves of the sulfur/SFCs composites are shown in Fig. 3(b), the specific capacity of 1223 mAh g^{-1} is obtained from the first discharge. The reversible specific capacity of the sulfur/SFCs composites is 400 mAh g^{-1} , it means the high utilization of the sulfur. The charge-discharge efficiency closes to 90% after the first cycle. The sulfur/SFCs composites with the structure of the interior and surface sulfur of the SFCs can effectively prevent the dissolution of sulfide. In the first discharge curve, there is an obvious plateau at 0.75V, which is the main reduction reaction of S reducing to S^{2-} and the formation of Li_2S in the electrode material [17, 18].

In the process of discharge, the Li is oxidized and forms the Li_2S , and the polysulfide (Li_2S_8 , Li_2S_4 , Li_2S_2) may be formed. Some polysulfide will dissolve into the electrolyte, which can not be oxidized to the sulfur. The reaction equations may be described as follows:



4. CONCLUSIONS

The sulfur/SFCs composites have been prepared by pyrolysis and hydrothermal method. The phase structure and morphology of the sulfur/SFCs composites is obviously changed by the synthesized sulfur during the hydrothermal process. The sulfur/SFCs composites with the structure of interior and surface sulfur of the SFCs exhibit good electrochemical performance. The initial discharge specific capacity is 1223 mAhg^{-1} and the reversible specific capacity of the sulfur/SFCs composites is about 400 mAhg^{-1} . The charge-discharge efficiency closes to 90% after the first cycle. The high specific capacity and excellent cycling stability are related to the high theoretical capacity of sulfur and the combination with the SFCs as the conductive agent.

ACKNOWLEDGEMENTS

This work was financially supported by the NSFC (51564009, 51468011 and 51463007), the NSF of Guangxi Province (2015GXNSFDA139035, 2014GXNSFAA118331, 2014GXNSFDA118006, 15-KF-8 and KH2013YB008)

References

1. P. G. Bruce, S. A. Freunberger, L. J. Hardwick, J. M. Tarascon, *Nature Materials*, 11 (2011) 19.
2. X. L. Ji, L. F. Nazar, *Journal of Materials Chemistry*, 20 (2010) 9821.
3. H. Yamin, A. Gorenshtein, J. Penciner, Y. Sternberg, E. Peled, *Journal of the Electrochemical Society* 135 (1988) 1045.
4. Y. Li, Y. W. Mai, L. Ye, *Composites Science and Technology*, 60 (2000) 2037.
5. S. Mishra, A. k. Mohanty, L. T. Drzal, M. Misra, G. Hinrichsen, *Macromolecular Materials and Engineering*, 11 (2004) 289.
6. I. D. Ibrahim, T. Jamiru, E. R. Sadiku, W. K. Kupolati, S. C. Agwuncha, G. Ekundayo, *Composite Interfaces*, 23 (2016) 15.
7. M. A. Khan, S. Guru, P. Padmakaran, D. Mishra, M. Mudgal, S. Dhakad, *Composite Interfaces*, 18 (2011) 527.
8. L. Xiao, Y. Cao, J. Xiao, B. Schwenzer, M. H. Engelhard, L. V. Saraf, Z. Nie, G. J Exarhos, J. Liu, *Advanced Materials*, 24 (2012) 1176.
9. N. Jayaprakash, J. Shen, S. S. Moganty, A. Corona, L. A. Archer, *Angewandte Chemie*, 20 (2011) 5904.
10. P. Yiseul, O. Misol, S. P. Jung, *Carbon*, 94 (2015) 9.

11. H. Yang, H. Wang, S. Ji, Y. Ma, V. Linkov, R. Wang, *Journal of Solid State Electrochemistry*, 18 (2014) 1503.
12. R. Du, Z. F. Tong, C. Wei, A. M. Qin, *International Journal of Electrochemical Science*, 11 (2016) 8418.
13. R. Du, Z. F. Tong, C. Wei, A. M. Qin, K. Y. Zhang, L. Liao, *International Journal of Electrochemical Science*, 11 (2016) 8581.
14. Z. S. Zhao, C. M. Li, W. K. Wang, H. Zhang, M. Y. Gao, X. Xiong, A. B. Wang, K. G. Yuan, Y. Q. Huang, F. Wang, *Journal of Materials Chemistry*, 10 (2013) 3334.
15. X. L. Cui, Z. Q. Shan, L. Cui, J. H. Tian, *Electrochimica Acta*, 105 (2013) 23.
16. P. G. Bruce, B. Scrosati, J. M. Tarascon, *Angewandte Chemie International Edition*, 47 (2008) 2930.
17. D. W. Wang, G. Zhou, F. Li, K. H. Wu, G. Q. Lu, H. M. Cheng, I. R. Gentle, *Physical Chemistry Chemical Physics*, 14 (2012) 6706.
18. S. Z. Xiong, K. Xie, Y. Diao, X. B. Hong, *Ionics*, 18 (2012) 867.

© 2017 The Authors. Published by ESG (www.electrochemsci.org). This article is an open access article distributed under the terms and conditions of the Creative Commons Attribution license (<http://creativecommons.org/licenses/by/4.0/>).